Vol. 340: 139–153, 2007 | MARINE ECOLOGY PROGRESS SERIES
Mar Ecol Prog Ser | Published June 18

Transport and degradation of a dinoflagellate bloom in permeable sublittoral sediment

Markus Huettel[1,3,*], Perran Cook[1,4], Felix Janssen[1], Gaute Lavik[1], Jack J. Middelburg[2]

[1]Max Planck Institute for Marine Microbiology, Celsiusstraße 1, Bremen 28359, Germany
[2]Netherlands Institute of Ecology (NIOO-KNAW), Korringaweg 7, 4401 NT Yerseke, The Netherlands

[3]*Present address:* Florida State University, Department of Oceanography, 1015 West Call Street, Tallahassee, Florida 32306-4320, USA

[4]*Present address:* CSIRO Land and Water, 120 Meiers Road, Indooroopilly 4068, Australia

ABSTRACT: Filtration of planktonic algal cells from the water column into permeable sublittoral sediment and the fate of the cells in the shallow sands were studied during a red tide produced by the dinoflagellate *Peridinella catenata* at Hel Peninsula/Baltic in May 2004. Advective porewater flows associated with ripple topography of the bed caused rapid transport of algal cells down to 5 cm sediment depth. Sedimentary concentrations of algal cells mirrored algal concentrations in the overlying water column with increases and decreases within the upper 3 cm of the bed occurring within a few hours. Sedimentary algal uptake and release significantly differed between stations only 15 m laterally apart. Laboratory sediment-column experiments with ^{13}C-labeled algal cells revealed algal decomposition at rates of up to 0.2 % ^{13}C h^{-1} in percolated sands originating from the study site. This was 2 orders of magnitude lower than observed decreases in sediment algal cell C abundance of up to 23 % C h^{-1} after a drop in cell concentrations in the water column. Because bioturbation and ripple migration were negligible, we conclude that advective flushing of the uppermost sediment layer could rapidly remove cells from the sediment. Our results demonstrate close spatial and temporal coupling between algal cell concentrations in the boundary layer and those in the upper 6 cm of permeable sand sediment, and suggest that permeable beds can act as short-term storage buffer for phytoplankton. During passage through the sediment, planktonic algae may benefit from the higher nutrient concentrations available in the porewater.

KEY WORDS: Advective transport · Permeable sediment · Phytoplankton bloom · Baltic · Red tide · *Peridinella catenata*

INTRODUCTION

Waves and strong bottom currents keep the surface layers of sublittoral sand sediments unconsolidated and highly permeable to water flow. Frequent sediment movement and resuspension prevents accumulation of fine materials and results in well sorted beds with relatively low organic content (Kranck et al. 1996). Such beds presently cover large sections of the world's shelf floors. In 1968, Webb & Theodor (1968) injected dye into sublittoral mediterranean sands and observed dye emergence at the ripple crests caused by the interaction of bottom flows and sediment topography. Riedl et al. (1972) buried flow sensors at 10 to 30 cm depth in nearshore sands (15 to 100 cm water depth, North American Shelf) and observed horizontal and vertical porewater transport velocities of up to 36 cm h^{-1}. These authors estimated that this porewater transport leads to an average exchange of 33.2 l m^{-2} d^{-1} in the shallow shelf (<200 m water depth). Since then, this exchange process has been confirmed by several research groups (Harrison et al. 1983, Ziebis et al. 1996, Falter & Sansone 2000, Precht & Huettel 2004, Reimers et al. 2004), with measured

*Email: mhuettel@ocean.fsu.edu

and calculated filtration rates of up to several hundreds of liters m^{-2} d^{-1}.

This relatively strong interfacial water flow has the potential to carry suspended small particles into the porous sand bed, and several flume and *in situ* experiments demonstrated that clay particles, fluorescent tracer particles and planktonic algae can be transported into the bed by the interfacial water flows (Packman & Brooks 1995, Huettel et al. 1996, Pilditch et al. 1998, Huettel & Rusch 2000, Packman et al. 2000, Packman & Brooks 2001). As oxygen enters the sediment with the same water flows as the particles, and degradation products are removed from the sediment by the porewater flows (Huettel et al. 2003), this filtration process also promotes a sedimentary environment that is supportive of efficient and rapid degradation of organic particles carried into the bed. According to studies by Kristensen et al. (1995), Kristensen & Hansen (1995), and Dauwe et al. (2001), the decomposition rate of a large fraction of organic matter buried in marine sands is accelerated by availability of oxygen. Synthesis of the listed findings suggests that shallow permeable shelf beds represent large biocatalytical filter systems that possibly have a strong influence on the cycles of matter in the shelf and coastal water quality.

Relentless coastal development and the rapid increase of the human population in coastal zones (Niemi et al. 2004) are associated with increased nutrient concentrations in nearshore waters that promote algal growth and blooms (Nixon 1995, Seitzinger & Kroeze 1998, Paerl et al. 2002). The frequency and duration of such blooms has been increasing since the onset of rapid industrial development (Nixon 1995, Howarth et al. 2002, Paerl et al. 2002, Glibert et al. 2006), stressing the potential importance of nearshore filtering, sand beds for the degradation of this organic material. Bed filtration may clear the water of toxic red tides, enhance water clarity necessary for benthic primary production promoting high oxygen concentrations at the sea floor, and may prevent the build-up of large amounts of organic material that can result in anoxic bottom boundary layers. Recent laboratory investigations (Lohse et al. 1996, Jahnke et al. 2005a) suggest that permeable shelf sands are sites of considerable denitrification activity; thus, such beds could effectively remove nitrogen from the coastal ocean and thereby counteract, to some extent, the effects of coastal eutrophication.

So far, the filtration of an algal bloom into permeable marine sediments has not been investigated *in situ*, and conclusions from flume experiments are limited due to restrictions in water depth, wave height, sediment depth, lack of fauna, atypical biogeochemical zonation, etc. Two *in situ* studies have measured degradation rates of artificial algal blooms in sandy sediments (Ehrenhauss et al. 2004a,b). A critical question is, whether algae advected into the sediment immediately begin to break down or if cells survive for a period of time before the onset of decomposition. In many decomposition experiments, dead algae are used as a carbon source, and the degradation status of the cells may mean that the responses observed in these studies are not directly representative of *in situ* conditions (e.g. Moodley et al. 2005). To our knowledge, no comparisons of the response of live and killed treatments exist in the literature. Also, continuous rapid interfacial porewater exchange may mean that filtered particulate organic matter can be lost from the sediment again, and no information is available on this process.

The aim of this study was to investigate the filtration and degradation of phytoplankton in shallow sublittoral sands with emphasis on the temporal and spatial characteristics of these processes. A dense dinoflagellate bloom developed close to Hel peninsula (Baltic, Poland) during a sequence of very calm, sunny days in late spring 2004. We used the dinoflagellate cells as natural tracer particles and model organisms for the quantification of filtration and sedimentary mineralization of algal cells. Algal counts along sedimentary transects permitted the assessment of deposition patterns and their spatial and temporal dynamics. Parallel laboratory experiments with labeled bloom dinoflagellates allowed quantification of the degradation rates of live and killed treatments and investigation of whether degradation can account for observed decreases in sedimentary algal cells.

MATERIALS AND METHODS

Study site. The study site was in shallow water (<1.5 m) with unvegetated sandy sediment located off the township of Hel on the Hel Penisula on the Baltic coast of Poland (54° 36′ 22″ N, 18° 48′ 00″ E; Fig. 1). The water is brackish with a salinity of 7, and water temperature during the study period at the beginning of May 2004 was 8°C. The sediment consists of well-sorted quartz sands with a median grain size of 210 µm. Sediment permeability was measured using constant-head permeametry (Klute & Dirksen 1986) in triplicate cores (3.6 cm diameter, 15 cm long) retrieved from the sampling sites. Tidal influence is minimal, and small changes in water depth at the site are controlled by wind-driven seiches. Flow velocities were measured with a Nortek™ acoustic Doppler velocimetry system (ADV), with the measuring volume positioned ~12 cm above the sediment surface. During the investigations, weather was very calm (winds < 2 m s^{-1}) and sunny.

Algal bloom sampling. In the morning of May 1, 2004, a dense bloom of the dinoflagellate *Peridiniella*

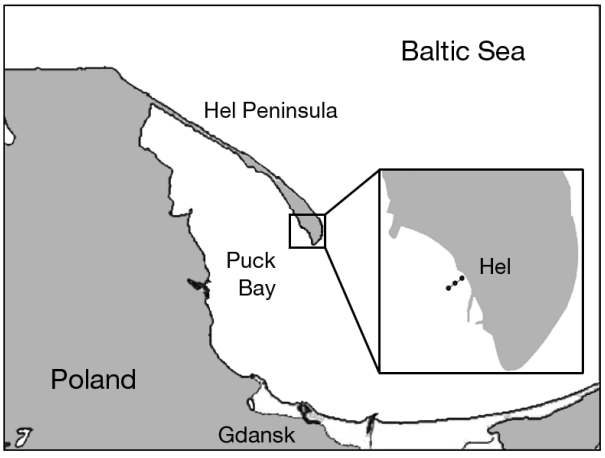

Fig. 1. Study site at Hel Peninsula, Poland. (●) 3 stations along seaward transect (0.5, 1.0 and 1.5 m depth, respectively)

catenata was carried into Hel Bay, where it concentrated in the shallow zone causing a reddish-brown appearance of the water (see Fig. 2). *P. catenata* blooms are considered non-toxic (Haya 1995), and no adverse effects on the fauna present at the study site could be observed. Water and sediment samples were collected throughout the day (at 09:30, 14:30, 17:00 and 21:30 h) at 3 stations located at 0.5, 1.0 and 1.5 m water depth along a transect extending in a southwesterly direction, perpendicularly from Hel beach (Fig. 1). Water was sampled in triplicates at 20 cm above the sediment surface using 50 ml centrifuge vials. Water samples taken at 09:30 h were lost during transport, however, from the turbidity and color of the water we assume that algal concentrations at 09:30 h were less than those at 14:30 h, when the color of the water had turned to an intense brownish-red. Sediment cores were collected in triplicate at ripple slopes using cut-off syringes (20 ml), and cut at 7, 15, 30, 45 and 60 mm intervals. The resulting sediment slices as well as the water samples were preserved in formaldehyde solution (4% final concentration). For algal counts, the sediment slices were resuspended and, immediately after sedimentation of the sand grains, 75 µl of the water overlying the sand was extracted with an Eppendorf pipette. Dinoflagellate cells in these subsamples and the water column samples were counted under the microscope.

Algal distribution on sediment surface. Algal cell deposition on the rippled surface of the Hel sediment affected by water filtration through the upper layers of the sand bed was investigated using image analysis of 6 close-up digital images taken from the sediment surface at the deepest station (1.5 m). Pictures were taken vertically downwards at 30 cm distance from the sand bed. Green light (500 to 550 nm) reflected from chlorophyll accumulated at the sediment surface was extracted from the images by spectral analysis with the image-processing software NIH-image. The surface deposition was further analyzed in a wave tank with sand of the same grain size and waves of similar dimensions. A 10 cm-thick layer of algae-free sediment was placed in a 6.1 m long, 31 cm wide, and 46 cm deep wave tank. Water depth in the tank was adjusted to 30 cm, and for a period of 10 min the wave paddle mounted at one end of the tank produced waves of 10 cm amplitude and a frequency of 1.2 Hz that generated a rippled surface (ripple amplitude 0.6 cm, wavelength 6.8 cm) on the incubated sediment layer. After this initial period, the waves were reduced to 2.5 cm amplitude, ~200 cm wavelength, at 0.6 Hz that caused oscillating flow at the sediment–water interface but no grain movement (maximum velocity at 10 cm above the bed was 10 cm s^{-1}). Then a suspension of dead phytoplankton cells (a mix of *Thalassiosira weissflogii*, *Pavlova* sp. and *Nannochloropsis* sp., 2.6×10^8 cells l^{-1} final concentration) was added to the water. After 24 h, the water was partly drained from the wave tank and the surface was photographed for image analysis as described above. Sediment cores (2 cm diameter, 5 cm long) taken in triplicates at the ripple slopes provided the reference chlorophyll data for the image analyses.

Algal distribution within Hel sediment. To assess the small-scale depth distribution of algae in the sandy sediment, 2 sets of 10 cut-off syringes (20 ml, 1.9 cm diameter) were pushed adjacent to each other into the sediment at the deepest station along 2 parallel small transects (20 cm long) perpendicularly crossing a ripple (2 cm amplitude, 20 cm wave length). The sediment cores were cut at 1.5 cm depth intervals, and slices of the same depth from the 2 replicate cores were pooled and frozen. Pigment (chlorophyll *a* [chl *a*], phaeophytin, total phaeopigment) distributions whithin the sediment were analyzed according to Strickland & Parsons (1972) using a 90% acetone extraction. Data were plotted with the software package 'surfer', revealing the two-dimensional distribution of chl *a* below the sediment ripple.

Organic matter labeling and degradation experiments. In order to assess the degradation rate of the algal bloom in the sediment, we performed percolation column experiments with labeled *Peridiniella catenata*. $H^{13}CO_3^-$ (~500 µM) was added to freshly collected water containing the bloom, which was then incubated for 2 d under natural daylight conditions and at *in situ* temperature. A portion of the labeled algal bloom was then frozen and thawed (hereafter referred to as 'the frozen treatment', with the unfrozen treatment hereafter referred to as 'live'). Samples from each treatment were collected onto Whatman GF/F filters for analysis of chl *a*, POC and ^{12}C:^{13}C ratios. Analysis of

the labeled algal bloom showed that the $\delta^{13}C$ of the POC reached ~1200‰ for the frozen treatment and ~2500‰ for the live treatment. We suggest 2 possible reasons for this difference: (1) The frozen treatment was made ~12 h before the samples were applied to the sediment columns and would have stopped assimilating dissolved inorganic (DI)^{13}C immediately; in the interim, the live treatment, would have continued to assimilate DI^{13}C (both in the dark and during limited periods of illumination) before the cells were applied to the columns. (2) Due to the freezing and thawing, some of the algal cells were destroyed, losing their cell contents (which were presumably more enriched in ^{13}C than the more rigid cellular components).

Eight acrylic core liners (36 mm internal diameter) were filled to a height of 5 cm with sieved sand collected from the study site at a water depth of 1.5 m. The sediment was sieved through a 0.5 mm sieve in order to remove macrofauna. Filtered site water (Whatman GF/F) was pumped from top to bottom through the cores at a rate of ~0.17 l d^{-1}, which was equivalent to a flushing rate of ~170 l m^{-2} d^{-1} and a porewater velocity of 1.8 cm h^{-1}. This flow rate ensured that the porewater was still oxic after having passed through the sediment columns, which was verified throughout the experiment by measurements of O_2 concentration in the outflow water of all columns. Experiments commenced with the addition of 100 ml (corresponding to approximately 2×10^5 cells or 560 µg C) of the live and frozen algal bloom treatments to 4 columns for each treatment. This is equivalent to the amount of algae that would be transported into the sediment during 1 d assuming a flushing rate of 100 l m^{-2} d^{-1} (the upper range of flushing rates at that site under calm conditions). Microscopic observations of the live treatment showed that the dinoflagellate cells were still alive upon addition to the column. After the addition of algae, the entire cores were immediately rinsed (10 ml min^{-1}) with ~200 ml of filtered site water to wash away unfixed bicarbonate label. The efficiency of this rinsing process was checked by flushing 2 'blank' columns with 500 µM $H^{13}CO_3$ only, followed by subsequent rinsing with site water as described above. The cores were then left to incubate under continuous flushing, and the core outlet water was sampled at ~24 h intervals to determine ^{13}C:^{12}C ratios of particulate organic carbon (POC), dissolved organic carbon (DOC) and dissolved inorganic carbon (DIC). Samples of reservoir water were also taken and processed simultaneously in the same way for determination of the background ^{13}C:^{12}C ratios of the POC, DOC and DIC fractions. After 2.5 d, 2 of the columns from each treatment were sacrificed and the sediment collected and frozen for later analysis of ^{13}C:^{12}C ratios of POC. After 5 d the remaining 2 columns for each treatment were sacrificed and sampled in the same way.

Samples for POC analysis were collected by filtering though 1 µm glass-fiber Millipore cartridge filters, the filtrate was collected for DOC analysis. Samples for DIC analysis were preserved with 0.01% $HgCl_2$ (final concentration). The ^{13}C:^{12}C ratios of POC samples were analyzed using a Finnigan Delta S isotope ratio mass spectrometer coupled on-line via a conflo interface with a Carlo Erba/Fisons/Interscience elemental analyzer. DIC ^{13}C:^{12}C ratio was analyzed using a gas chromatograph coupled to a continuous flow GC-IRMS (VG Optima). The ^{13}C:^{12}C ratio of DOC was determined as DIC after a persulfate digestion as described by Menzel & Vaccaro (1964). The excess ^{13}C in each sample was calculated by subtracting the background ^{13}C:^{12}C ratio determined in the sediment (POC), reservoir (DOC) and blank columns without algae addition (DIC). A natural abundance $\delta^{13}C$ of –20‰ was assumed for the phytoplankton, any errors arising from this assumption are likely to be negligible given that the enrichment of the algal associated POC was in excess of 1000‰. POC was analyzed after acidification using a Fisons NA1500 elemental analyzer.

A rate constant for organic matter degradation was estimated from a fit of the data to the equation $G(t) = Ge^{-kt}$, where $G(t)$ is amount of labeled POC at Time t (estimated from the initial amount of excess ^{13}C minus the cumulative loss of $^{13}CO_2$), and k is the first-order decay constant. This differs from the conventional bi-exponential fit, which identifies 2 reactive and 1 non-reactive fraction of organic matter (e.g. Westrich & Berner 1984); however, the short-term incubations conducted here only allow the first (labile) fraction of organic matter to be resolved.

RESULTS

In situ observations and flume experiment

May 1, 2004, was a very calm day in Hel Bay. At 09:30 h the water was smooth with surface wave amplitudes <10 cm, and the green color of the water indicated the presence of a phytoplankton bloom. A weak coastal current carried a red tide into Hel Bay leading to increased turbidity, and by 14:30 h, the water close to the beach (<3 m depth) had become reddish-brown caused by massive occurrence of the dinoflagellate *Peridiniella catenata* (Fig. 2) reaching an average (±SD) of 4.9 (± 0.3) $\times 10^6$ cells l^{-1} or 80 µg chl *a* l^{-1} at the shallowest station (0.5 m). At the 2 deeper stations, concentrations were lower (1.0 m station: 2.1×10^6 cells l^{-1}; 1.5 m station: 1.1×10^6 cells l^{-1}). During the afternoon, algal abundances in the water column decreased but remained higher than 0.49×10^6 cells l^{-1} throughout the rest of the day.

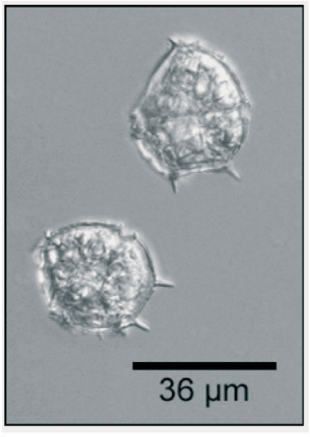

Fig. 2. Water at Hel beach stained by red tide caused by dinoflagellate *Peridiniella catenata* (lower panel, identified and photographed by Dr. Jozef Wiktor, Marine Ecology Department, IOPAS, Poland)

F. Wenzhoefer et al. unpubl.), very similar to flow patterns observed in laboratory wave tank experiments (Precht & Huettel 2003). These interfacial flows filtered suspended *Peridiniella catenata* (diameter 34 to 37 µm) (Figs. 2 & 4) and cells that were deposited onto the bed surface into the permeable sediment. A large fraction of the algae was trapped in the uppermost sediment layer (0 to 7 mm). Algae concentrations were highest in the ripple troughs and ripple slopes, where water flow into the sediment was strongest (Fig. 3a). The wave tank experiment, producing very similar distribution patterns of algae in the sediment surface layer, supported the hypothesis that the chlorophyll pattern on the rippled surface observed in the field was caused by wave-induced transport of algal cells into the surface layer (Fig. 3b,c). Likewise, the 2-dimensional chlorophyll plot produced from the transect measurements over the ripple reflected this algal distribution, with maximum values in the upper ripple slopes and the ripple troughs. The chlorophyll signal produced by *P. catenata* filtered into the bed exceeded the chlorophyll contained in benthic diatoms and detritus particles, which reached 1 µg g^{-1} in the uppermost sediment layer. Due to the oscillating flow direction, which forces algal cells into the slopes, the concentration maxima on both sides of the ripple crest can join to form high concentrations of algae at the ripple crest. Phaeopigments reached highest values below the surface of the ripple troughs, at 0.5 to 2.5 cm sediment depth (Fig. 4).

The ADV measurements obtained at ~12 cm above the sand bed showed steady bottom currents in an approximately northerly direction (almost paralleling the beach) with velocities of less than 4 cm s^{-1} overlaid by wave-induced orbital velocities of less than 7 cm s^{-1} aligned roughly perpendicular to the shoreline (Table 1). These bottom currents were sufficient to generate water flow through the upper sediment layer. Average permeabilities (±SD) for the upper 10 cm of the sediment were $3.74 \pm 0.28 \times 10^{-11}$ m^2 at 0.5 m, $3.46 \pm 0.20 \times 10^{-11}$ m^2 at 1 m, and $2.77 \pm 0.08 \times 10^{-11}$ m^2 at 1.5 m water depth, permitting advective porewater flow through the upper layer of the bed. Injection of fluorescent tracers and measurements with planar oxygen optodes revealed porewater flows from the ripple troughs to the ripple crests (Cook et al. in press, F. Janssen et al. unpubl.,

Table 1. Steady and oscillating flow velocities (averaged over measurement duration) at study site during our investigation. Velocities for oscillating flows are averages of absolute values of orbital flow velocities; flow direction is given in degrees on compass scale. Measurements conducted with an acoustic Doppler velocimetry system. Start: time of day experiment began; Duration: measurement duration; Distance: distance to sediment, i.e. depth at which volume was measured

Date (2004)	Start (h)	Duration (min)	Distance (m)	Steady flow (cm s^{-1})	(°)	Oscillating flow (cm s^{-1})	(°)
1 May	15:28	70.0	0.12	3.0	336	2.6	46
	20:20	70.0	0.12	1.2	13	2.0	50
2 May	01:11	70.0	0.12	1.7	322	2.0	43
	06:03	68.1	0.12	2.6	304	2.8	45
	23:28	70.0	0.12	1.4	292	3.1	48
3 May	04:20	67.0	0.12	2.8	304	2.8	40
	09:11	70.0	0.12	2.1	301	6.9	32
	14:03	70.0	0.12	0.7	265	3.8	42
	18:53	110.0	0.12	1.1	102	1.0	45
	21:49	95.4	0.12	1.8	214	1.1	51
4 May	03:11	93.9	0.12	2.3	288	1.6	39
	12:28	66.4	0.11	3.7	321	5.4	37
	17:20	70.0	0.11	1.7	304	6.3	40
	22:11	67.1	0.11	0.9	36	2.7	39
5 May	03:03	70.0	0.11	1.7	322	4.4	40

The sedimentary cell-count time series revealed temporal and spatial variations within the 30 m-long transect during the course of the day (Fig. 5). At 09:30 h, cell abundances, integrated over the upper 6 cm of the sediment, were significantly different (Mann-Whitney *U*-test, $\alpha = 0.1$) between the 0.5 m station and the other 2 stations (only 15 and 30 m away). Depth-integrated cell abundances changed during the day, with different temporal developments between stations. Highest abundances were recorded at 14:30 h at the 0.5 m station (28×10^6 cells m^{-2}), decreasing within 2.5 h to 12×10^6 cells m^{-2}. In contrast, abundances at the 1.5 m sta-

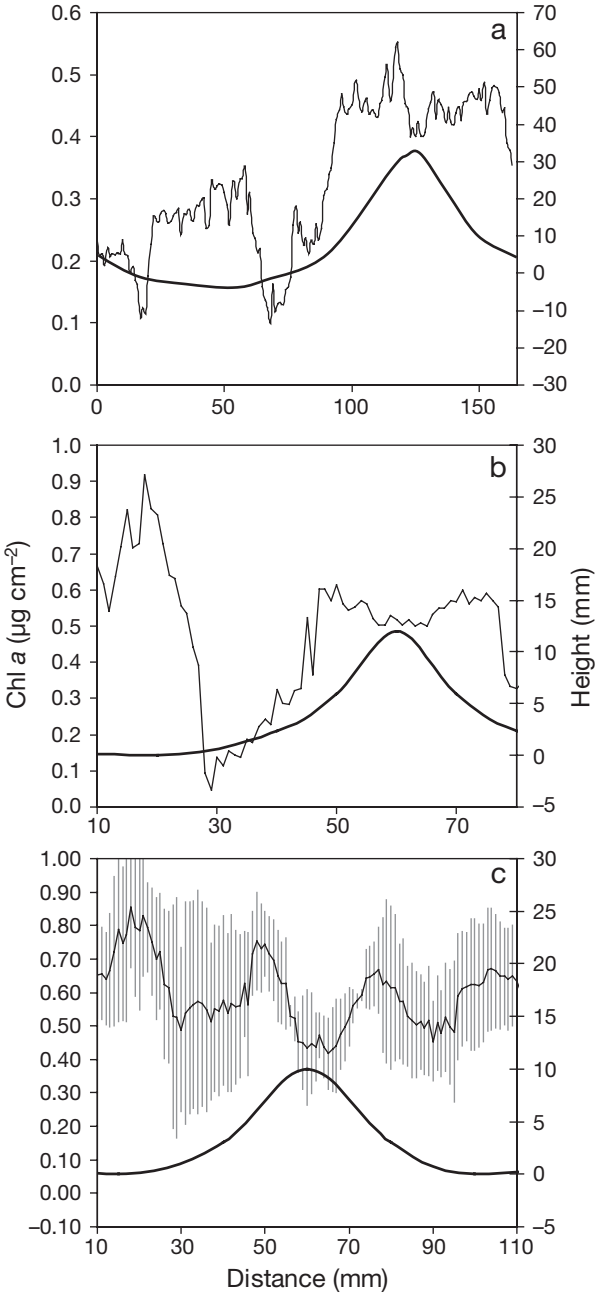

Fig. 3. Algal cell deposition pattern at sediment surface (a) in the field and (b,c) in the wave tank, assessed by image analysis of sediment surface color. The wider image used for the analysis in (c) shows the deposition pattern over one ripple wave length. Thick black line: height of sediment surface; gray bars in (c): SD (n = 4)

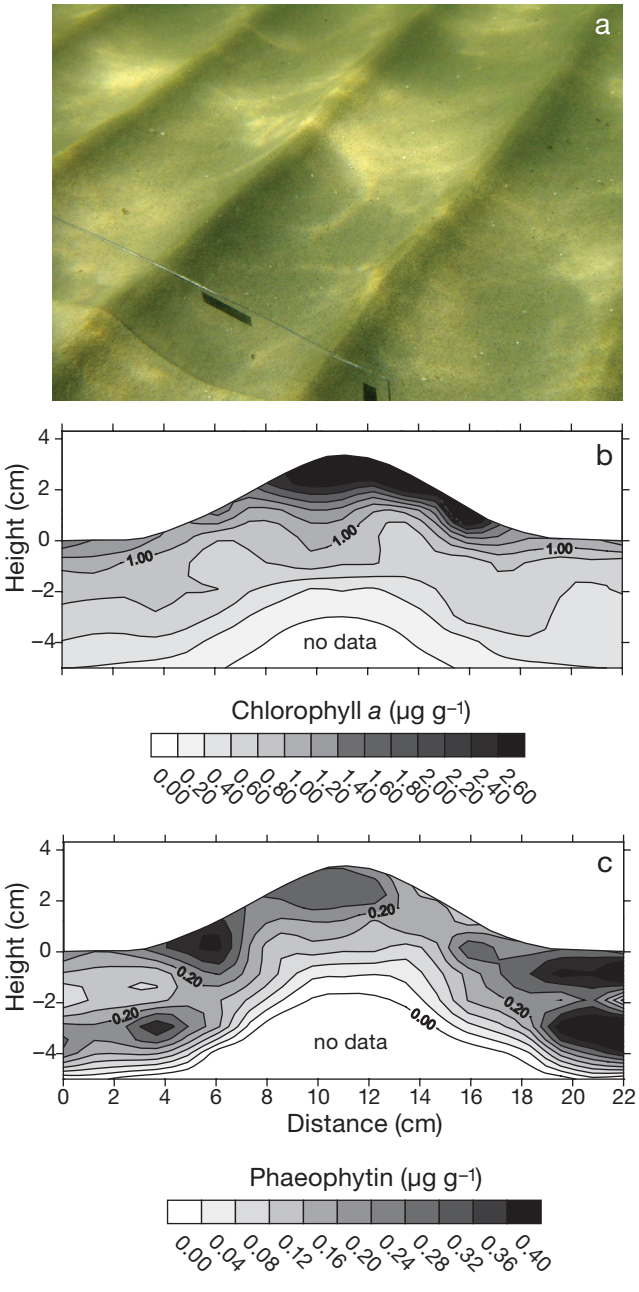

Fig. 4. *Peridiniella catenata*. (a) Algal cell concentration at ripple slopes and crests producing greenish-brown ripples; (b,c) 2-dimensional distribution of (b) chlorophyll *a* and (c) phaeophytin under sediment ripple at Hel (1.0 m station) (white area below ripples was beyond reach of the sampling syringes, thus there are no data for this area)

tion increased after 09:30 h within 5 h, from 8.8 to 24 × 10^6 cells m^{-2}, and remained more or less constant after 14:30 h. Likewise, cell abundances at the middle station at 1 m depth almost doubled between 09:30 h (4.5 × 10^6 cells m^{-2}) and 14:30 h (8.6 × 10^6 cells m^{-2}).

A closer look at the different sediment layers (Fig. 6) reveals that the observed changes in depth-integrated abundances were dominated by cell concentration changes in the surface layer (0 to 7 mm) that contained 75 ± 7% (0.5 m station), 70 ± 11% (1.0 m) and 88 ± 9% (1.5 m) of all algae (averages for all samplings). Below this layer, a consistent temporal pattern in the next 3 layers (7 to 15, 15 to 30 and 30 to 45 mm) showed increasing *Peridiniella catenata* abundances after 09:30 h, reaching peak values at 14:30 h and dropping to minimum abundances at 17:00 h. The occurrence of this pattern at all 3 stations indicated that a larger-scale process was responsible for the changes in algal abundance in the subsurface layers. This is supported by the comparison of the development at the 3 stations over time. Plotting the changes of algal concentration h^{-1} for the time period between 09:30 and 14:30 h, shows that cell abundance at the 1.5 m station in all layers increased faster than at the 1.0 m station and than cell abundance in most layers at the 0.5 m station (Fig. 7). Between 14:30 and 17:00 h, cell abundance declined in all layers at all stations except in the surface layer of the 1 and 1.5 m stations, but now with steepest hourly decreases at the 0.5 m station (–379 cells cm^{-3} h^{-1}). After 17:00 h, changes in sedimentary cell abundances were small (<33 cells cm^{-3} h^{-1}), except in the surface layer where abundances decreased at the 1 m

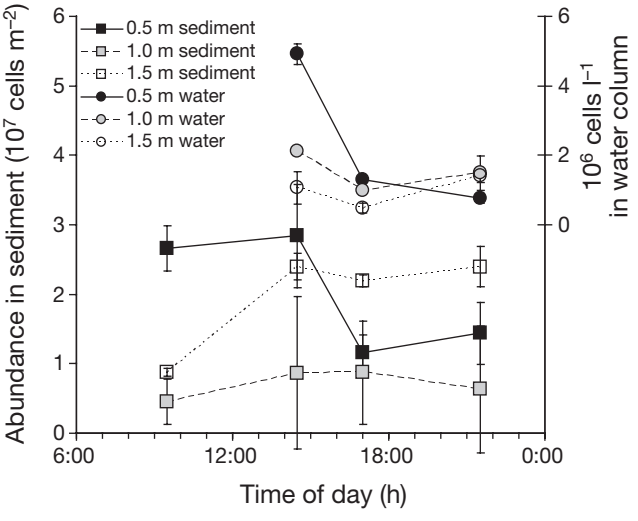

Fig. 5. *Peridiniella catenata*. Changes in algal cell numbers integrated over upper 60 mm of sediment, and algal concentrations in overlying water column, over time. No data available for water at 09:30 h. Error bars: SD

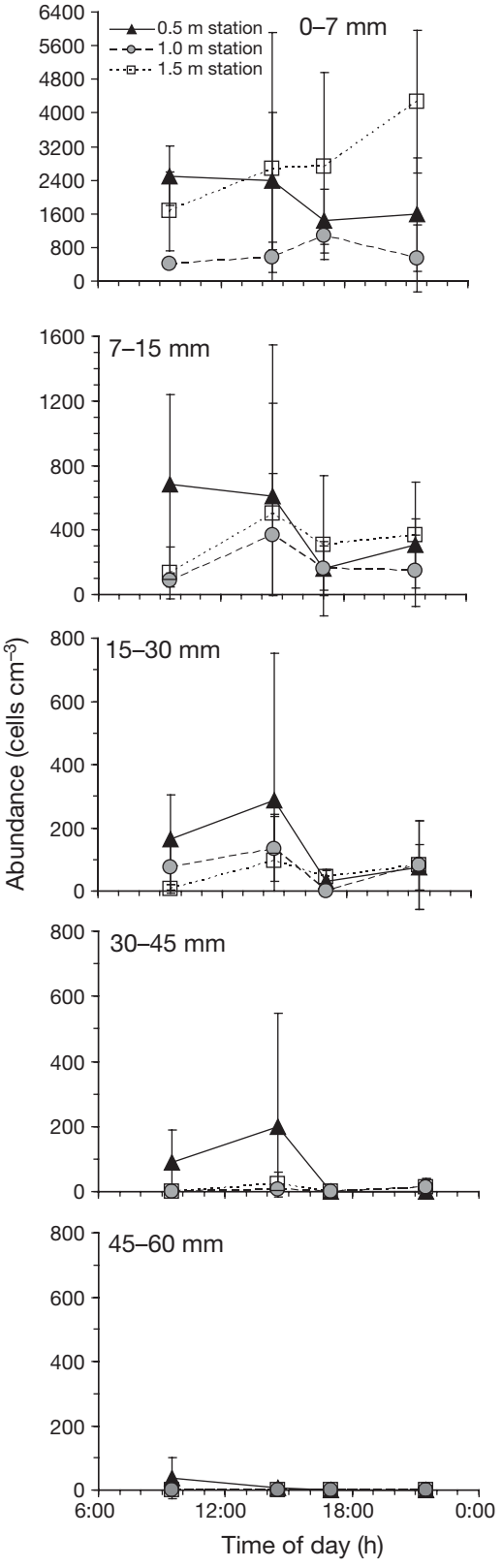

Fig. 6. *Peridiniella catenata*. Changes in algal abundance at different sediment depths over time. Note different *x*-axis scaling in the 2 uppermost graphs. Error bars: SD

station while increasing at the 1.5 m station. Maximum penetration depths of *P. catenata* cells into the sediment (defined as the depth where cell counts dropped below 1 cell cm^{-3}) ranged between 37 (1 and 1.5 m stations) and 52 mm (0.5 station) but did not show significant changes over time.

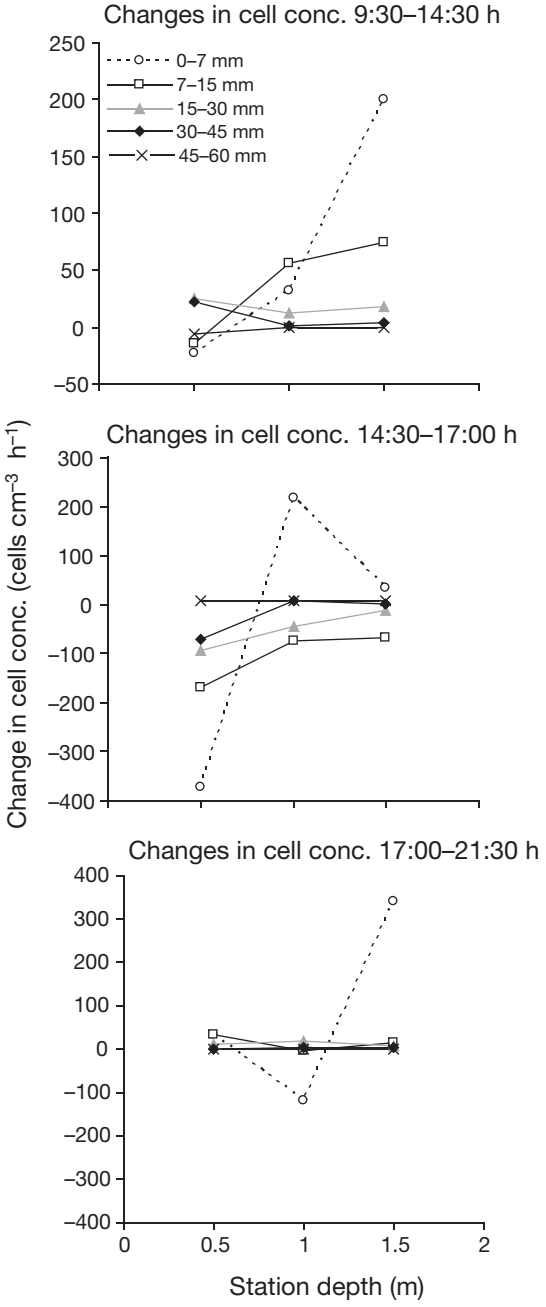

Fig. 7. *Peridiniella catenata*. Changes in algal cell concentration in different sediment layers at the 3 sampling stations. Between 09:30 and 14:00 h, algal concentrations increased in most layers at all stations; the opposite was found between 14:30 and 17:00 h, when concentrations dropped in most layers. Between 17:00 and 21:30 h, concentration changes were minor except in surface layer (0 to 7 mm)

Sediment column experiment

The sediment column experiment showed that the variations in algal abundances in the sediment could not be explained by decomposition of cells. After initial higher turnover rates lasting approximately 48 h (<5% ^{13}C d^{-1}), DIC, DOC and POC measurements indicated low degradation rates (<2% ^{13}C d^{-1}). In contrast, decreases in cell numbers in the sediment measured at the study site reached 23% C h^{-1} (0.5 m station, 14:30 to 17:00 h). DIC was consistently the dominant form of ^{13}C lost from the sediment column, with turnover rates of between 1.5 and 4% of added ^{13}C d^{-1} (Fig. 8). At 32 h, the frozen treatment had a slightly higher label-turnover rate than the live treatment; however, the turnover rates were essentially the same thereafter. The loss of label as DOC was highest at the start of the incubation, when ~3 to 4% of the label was lost in this form. As for DIC, the frozen treatment had a slightly higher loss of DOC than the live treatment initially, but it was essentially the same in both treatments thereafter. The loss as DOC dropped consistently for both treatments before peaking again at 80 h, and then becoming undetectable for the remainder of the experiment. The loss of label as POC varied between 1 and 2.5% d^{-1} at the start of the experiment, before dropping to ~0.5% for the remainder of the experiment. In contrast to DIC and DOC, the highest loss of POC occurred in the live treatment, and was observed consistently over the course of the experiment. This may suggest that cell motility plays an important role in the mobility of algae through permeable sediments. The first-order rate constants estimated for the algal cell degradation in the sediment were 7.6 and 9.6 yr^{-1} for the live and frozen cells, respectively.

Total recovery of label (POC in the column + POC washed out + DIC + DOC) was close (within 25%) to that estimated to have been added to the sediment column. Microscopic observations showed that the water that passed through the column during the rinsing step contained relatively few algal cells; thus, most of the added algae were retained within the columns. Furthermore these observations indicated that the algal cells that passed through the column were no longer motile, and were possibly damaged or dead. The blank columns showed that the added $H^{13}CO_3$ label became indistinguishable from the background after 20 h.

DISCUSSION

The *Peridiniella catenata* bloom at Hel beach produced natural tracer particles that could clearly be distinguished from other organic material in the sediments, and thus, provided an opportunity to investigate the

fate of a plankton bloom in a shallow environment with permeable sediment. Our study showed that the deposition and incorporation of the cells into permeable sand sediment is a rapid process and highly dynamic in space and time. Algal abundance in the upper sediment layers was coupled to the algal concentration in the overlying water column. Significant changes in sediment algal numbers occurred within time periods of less than 8 h, during which the total algal cell counts within the upper 6 cm of the sediment decreased by a factor of 2.3 (0.5 m station) or (only 30 m further seaward) increased by a factor of 2.4 (1.5 m station). Such changes in sediment labile organic matter content may have substantial impact on organisms and biogeochemical cycles in the metabolically most active surface layer (Rusch et al. 2001, 2003). Below, we address in sequence interfacial transport, ensuing algal cell distribution patterns, sedimentary decomposition and potential consequences of the observed processes.

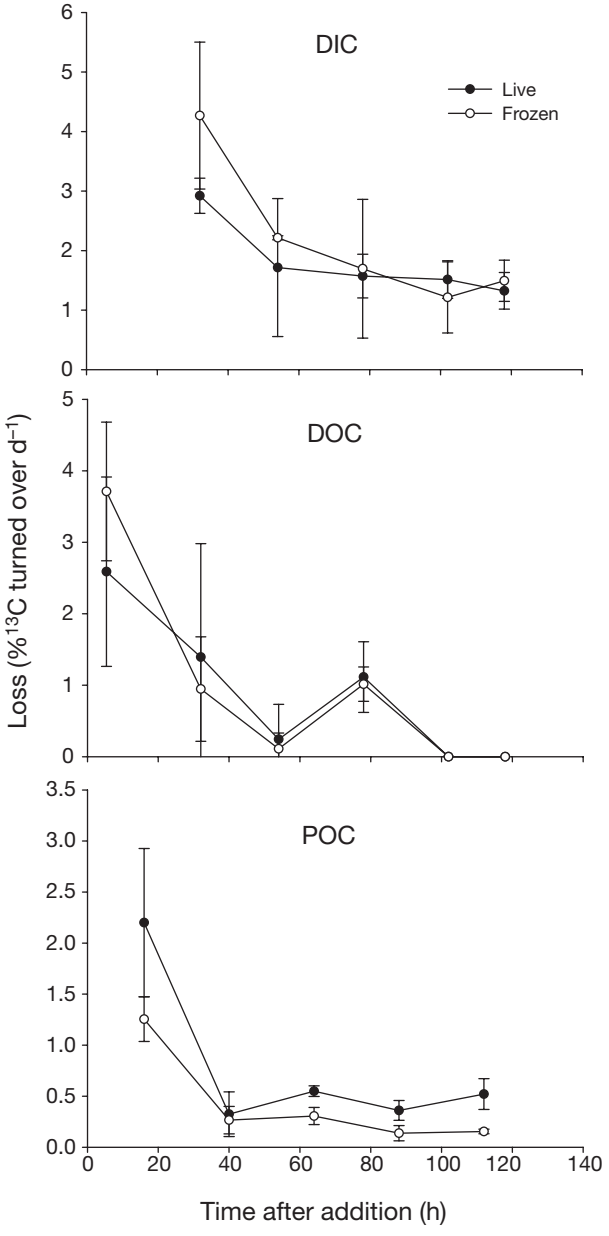

Fig. 8. *Peridiniella catenata*. Daily loss of ^{13}C in form of dissolved inorganic carbon (DIC), dissolved organic carbon (DOC) and particulate organic carbon (POC) from live and frozen ^{13}C-labeled dinoflagellate algae added to flushed sand columns. Error bars: SD of replicate columns (n = 4) for data points between 0 and 70 h, and range between 2 data points for times after 70 h

Advective porewater transport

Because of the very calm weather during our study period, wind- and wave-induced currents were weak and average flow velocities above the sand bed did not exceed 10 cm s^{-1}. Even such low currents have been shown to be effective in causing porewater flows in porous sediment when its permeability is high (Huettel & Gust 1992). The latter was the case in Hel, where sediment permeabilities of 3 to 4 × 10^{-11} m^2 resulted in filtration of water through the upper layers of the bed when bottom flows interacted with sediment topography in the shallow sublittoral. The dominant topography at the sampling stations was sediment ripples with an average wave length of 115.6 ± 28.5 mm and an average height of 17.5 ± 5.1 mm (measured by laserline surface scans, F. Janssen et al. unpubl.) that were formed by waves during less calm weather conditions prior to our study period. For ripples of such dimensions on sand beds, the penetration depth of flow-induced porewater circulation reaches down to a depth corresponding to half the distance between 2 adjacent ripple crests (i.e. 40 to 70 mm) (Huettel & Webster 2000), which agrees with the measured maximum algal penetration depth of 10 to 52 mm. The boundary currents forced fluid and suspended algae into the upper slopes of the ripples and the ripple troughs, as reflected by the chlorophyll distribution in the sediment surface layer (Fig. 3) and the 2-dimensional distribution of chlorophyll under the ripple (Fig. 4).

Distribution at sediment surface

In contrast to gravitational settling of organic particles onto the seafloor, which results in either a uniform distribution of that material or, when ripples are present, an accumulation of the material in the ripple troughs (Danovaro et al. 2001), filtration of algae into the surface of permeable sediments also produces particle concentration maxima in the upper ripple slopes, where the inflow of water into the sediment is

strongest (Huettel et al. 1996). When the filtration is caused by oscillating bottom flows (as generated at Helby small surface gravity waves), particles penetrate into both sides of the ripples, as also observed in our flume experiment (Fig. 3). If the ripples are stationary, these 2 particle accumulation zones may join to produce 1 zone of high particle concentration that includes the entire upper part of the ripple (Fig. 4). While chl *a* (indicative of fresh algal material) was concentrated in the ripple crest, phaeopigments, produced when chlorophyll is decomposed, reached highest concentrations at the base of the ripples and in the ripple troughs. This suggests that dead phytoplankton accumulated and degraded mostly in the ripple troughs, while fresh or living plankton cells were filtered by the ripples from the water column. This agrees with findings of Danovaro et al. (2001), who reported a similar distribution of chl *a* and phaeophytin in Mediterranean sediment as we observed in the Baltic, and also found highest glucosidase activity and highest bacterial cell divition rates in the ripple troughs. Dead phytoplankton tends to form aggregates in the water column (Jones et al. 1998, McCandliss et al. 2002). These larger particles with higher sedimentation rates are too large to be filtered into the sand and thus accumulate in the ripple troughs, as observed after plankton blooms (Jago & Jones 1998).

Depth distribution

When algal blooms are washed ashore, highest cell concentrations are reached in the shallowest water (Tomlinson et al. 2004, Hu et al. 2005). The surface-layer cell counts for our 3 stations indicate that the maximum deposition of algae moved from the shallowest towards the deepest station during the day. The layers below the surface layer show peak abundance at midday (14:30 h, Fig. 6), which was also the time with the highest algal concentrations in the water column. *Peridiniella catenata* cells were found down to 37 mm (1 and 1.5 m stations), and 52 mm sediment depth (0.5 m station) revealing a rapid vertical transport process. Flume studies conducted by Pilditch et al. (1998) and Huettel & Rusch (2000), showed that microalgae are carried several centimeters deep into permeable sands of similar permeabilities by interfacial fluid flows associated with bottom topography. The relatively rapid interfacial transport processes in the rippled sand bed produced a tight spatial and temporal coupling between algal cell concentrations in the water column and the sediment. After the first sampling at 09:30 h on the morning of May 1, 2004, the red tide that moved into Hel Bay caused algal cell concentrations at the 1 and 1.5 m stations to increase in all sediment depths down to 30 mm. At the shallowest station (0.5 m), where the small waves had the strongest influence on sediment filtration, algal cell concentrations at that time had already reached their maximum in the upper sediment layers (0 to 6, 7 to 14 mm) and concentrations in these layers dropped after 09:30 h. However, in the 15 to 30 mm depth layers, algal concentration at the 0.5 m station increased between 09:30 and 14:30 h, consistent with the trend observed at the other 2 stations. After 14:30 h, coastal currents carried the algal bloom out of Hel Bay, and the ensuing decline of algal cell concentrations in the water column was paralleled by a decrease in the algal concentrations in the subsurface sediment layers at all 3 stations (Figs. 6 & 7). While it is clear how the rapid increase of *P. catenata* in the sediment was caused by co-transport of fluid and suspended algae into the bed, the question arises as to which processes are responsible for the rapid decreases of algal cells in the sediment after 15:00 h.

Column experiment on algal degradation

The potential contribution of degradation processes to the change in algal abundance in the sediment was investigated in the laboratory column experiment. Whether organic matter degradation occurs under oxic or anoxic conditions has been shown to have an impact both on the degradation rates of algal material and the relative importance of DOC and DIC release (Kristensen & Hansen 1995, Kristensen et al. 1995, Andersen 1996). Therefore, a key question is whether the sediments in the field remained oxic throughout the region of cell decomposition, as was the case in our sediment column experiments. Oxygen profiles measured at the site revealed the presence of oxygen on average down to 2 cm, and at times down to 10 cm. Optode measurements showed O_2 intrusion into the ripple slopes and troughs (Cook et al. in press), similar to sedimentary oxygen distribution patterns observed in a wave tank (Franke et al. 2006). Given that the areas of O_2 intrusion in the ripple slope and trough are also the zones of greatest phytoplankton transport into the sediment, it seems likely that much of the phytoplankton degradation in the field occurred under oxic conditions within the sediment. In order to ensure that the columns remained fully oxic, water was pumped through the cores at a rate equivalent to a flushing rate of ~170 l m^{-2} d^{-1}, which is almost twice as high as the upper rate of flushing measured at the site (100 l m^{-2} d^{-1}). Because we could measure flushing rates in the field only under very calm conditions, a doubling of the rate in the experiment does not represent an unnatural setting and is supported by measurements in similar sublittoral sediments (Precht & Huettel 2004). Higher

flushing rates, however, also increase the decomposition rate, due to a better supply of electron acceptors to the microbial community and a more efficient removal of decomposition products that may have an inhibitory effect (Huettel et al. 1998).

In the column degradation experiment, the degradation rates of the live and frozen algal cells within the sediment were essentially the same. Microscopic observations of algal cells that were added as living cells and that had passed through the column revealed that most discharged cells were immobile and probably started to degrade immediately. Thus, the sediment response time and degradation rate of organic matter was most probably the same, irrespective of whether live or dead cells from the bloom were transported into the sediment.

Previous chamber experiments on transport and degradation of phytoplankton in permeable sediments (Ehrenhauss & Huettel 2004, Ehrenhauss et al. 2004a,b) consistently found an uptake of DOC by the sediment when freeze-dried diatoms and their associated DOC (released during freeze-drying) were added, suggesting that the microflora inhabiting permeable sediments can effectively assimilate DOC derived from algal cells. The data from our study indicated that initial DOC release from the sediment may approach that of DIC, but that the relative DOC loss drops rapidly after 1 to 2 d. Bacteria within permeable sediment are able to rapidly utilize the DOC released during decomposition before it is transported out of the sediment by advective porewater movement. Other similar studies conducted in sediments under diffusive conditions have also shown that the relative DOC loss from the sediment is generally very low compared to that of DIC (Andersen 1996, Burdige & Zheng 1998, Pedersen et al. 1999), except for short periods immediately following labile organic matter inputs (Andersen 1996, Pedersen et al. 1999). Thus, our data suggest that relatively little of the algae degraded in the permeable Hel sediments was released as DOC, rather, it was mostly mineralized to DIC within the sediment.

The decay constants measured in this study (7.6 and 9.6 yr^{-1}) are within the lower range of constants reported in studies reviewed by Westrich & Berner (1984). In coastal sediments, average Q_{10} values of 3 are typically observed (e.g. Middelburg et al. 1995, and Moodley et al. 2005 reported that the Q_{10} of freshly added algal material was 5). Therefore, it is conceivable that our reaction constants measured at 8°C would increase to ~23–29 yr^{-1} (assuming a Q_{10} of 3) or possibly higher at 18°C. Such values are in close agreement with decay constants of ~25 yr^{-1} for the oxic decomposition of the labile fraction of phytodetritus at similar temperatures measured by Andersen et al. (1984) and Westrich & Berner (1984).

Nevertheless, the sediment column experiments showed that algal decomposition within the sand sediment was too slow to explain observed rapid decreases after 14:30 h, suggesting that physical transport processes caused the rapid changes in algal abundance. During the study period, macrofauna abundances were low at our field site (141 ± 25 small polychaetes m^{-2}), and significant sediment transport did not take place during the very calm period of our investigation (ripples were stationary, erosion threshold for sediment of this grain size distribution is >20 cm s^{-1}; Amos et al. 1997, Widdows et al. 2004). A time series of topography measurements performed 2 d after our study but under the same calm conditions revealed hardly any ripple movement within 15 h (F. Janssen unpubl.). However, algal cells penetrated 5 cm into the sediment at the study site and were also flushed from the laboratory sediment columns showing that *Peridinella catenata* could be transported through the sediment. We conclude that at our field site advective flushing also removed algal cells from the surface sediment layer after cell concentrations decreased in the water column. We suggest that this occurred because the majority of the cells concentrated in the upper 2 cm of sediment and mostly near the ripple crest (Figs. 4 & 6). The upwelling of porewater under the ripple crest (Precht & Huettel 2003) pushes the particles that are forced horizontally into the ripple slopes upwards towards the surface, increasing cell concentration in the ripple crests that was visible as greenish-brown coloration of the crests (Fig. 4). Because the area where water penetrates the sediment (ripple troughs and slopes) is much larger than the release area (ripple crests), the upwelling porewater velocity under the ripple crests exceeds that of the intruding water flow (for mass balance, the volume of inflowing water must equal the volume of the water released from the bed). Upward flow through the algal cell accumulations at the ripple crests probably released *P. catenata* cells to the water column. Algal cells may survive the passage through the sediment and possibly benefit from higher nutrient concentrations in the upwelling porewater while moving through the sediment pores (Fig. 9).

Organic matter and chlorophyll *a*

Using the conversions as in Sims (1993), Verity et al. (1993) and Menden-Deuer & Lessard (2000), each *Peridiniella catenata* cell contained approximately 580 pg N, 140 pg chl *a*, and 2800 pg C. The highest *P. catenata* concentration in the sediment measured at the 1.5 m station at 21:30 h was 4267 ± 1697 SD cells ml^{-1} sediment or 2800 ± 1100 cells g^{-1} dry sediment. This corresponds to 0.39 ± 0.16 µg g^{-1} chl *a* g^{-1} dry sediment or to

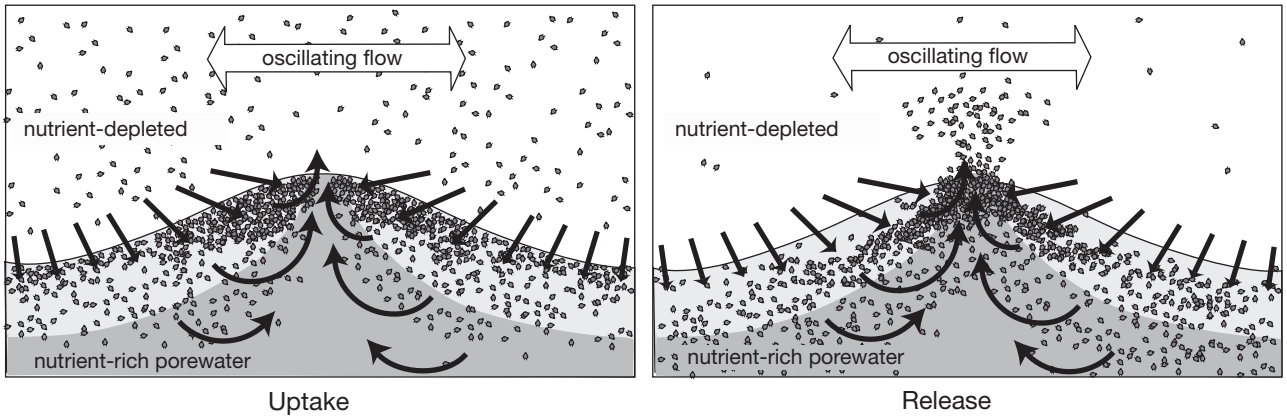

Fig. 9. Uptake and release of algal cells in permeable sediment. Black arrows depict interfacial and sedimentary water flows. Alternating with oscillating bottom-flow direction, cells are pushed into left or right slope of ripple. Near crest, cells from both sides may form a joint maximum. Algal cells that are filtered into permeable sand close to crest of ripple can be released again from sand bed after following a short curved path through the sediment. Within porewater upwelling zone (darker gray), algae are exposed to increased nutrient concentrations; however, large fraction of cells die and are degraded within sediment

15 to 40% of the chlorophyll found in the sediment surface layer, which explains the distinctive chl *a* pattern caused by algal filtration. Some of the pattern may have evolved from the migration of motile diatoms towards the zone of nutrient-rich porewater upwelling under the ripple crest (Huettel et al. 1998). However, the majority of diatoms in sandy sediment lives firmly attached to the sand grains, and the wave tank experiment — in which no benthic diatoms were present — demonstrated that the observed sedimentary chlorophyll distribution can be produced by pelagic algae filtration only (Fig. 3). The flow-induced filtration of algae, thus, produces ripple-parallel zones of enhanced organic matter deposition, which may influence organism and nutrient distributions in the sand. Since the algal cell-deposition zones are also the zones of oxic water penetration into the bed, these zones can be expected to be hot spots for organic matter decomposition and nutrient mobilization.

During the calm study period, the sediment filtered between 20 and 100 l m^2 d^{-1} (Cook et al. in press, F. Janssen et al. unpubl.) with the highest filtration rates reached at the shallowest station. Given the algal cell concentration in the water column (between 0.5 and 5 million cells l^{-1}), the cell concentrations measured in the upper 6 cm of 1 m^2 sediment could be reached within 3.6, 2.5 and 14.0 h for the 0.5, 1.0 and 1.5 m stations, respectively (based on 14:30 h sedimentary and water-column cell concentrations and a filtration rate of 40 l m^2 d^{-1}). This agrees with our observations of the movement of the red tide through Hel Bay and associated increase of *Peridiniella catenata* cell abundances in the sediment. During the 4 h before 14:30 h, the filtered algal cells accumulated organic carbon in the sediment corresponding to 0.1 to 0.5% of the average total organic carbon content (0.02 to 0.1% of dry weight) of the upper 6 cm of the sand bed. Although these percentages may appear low, they have to be related to the short time period of this uptake process and the processes that removed cells from the sediment. After the initial increases, the algal cell abundances in the sediment showed rapid decreases in the afternoon of May 1, 2004, in response to the decline of algal concentrations in the water column (Fig. 5).

These relative rapid fluctuations in the algal cell content of the sediment, which have to be attributed mostly to advective transport of cells into and out of the bed, emphasize the importance of factors that control retention of organic particles in permeable sediments. While the majority of algal cells were retained in the experimental sediment columns, which were flushed at porewater velocities exceeding *in situ* flushing rates by a factor of 2 or more, approximately 60% of the trapped algae were lost from the sediment at the 0.5 m station between 14:30 and 17:00 h when algal concentrations dropped in the water column. This apparent contradiction in retention efficiencies of the same sediment can be explained by the different pathways of the algae through the sediments. While in the columns algal cells had to travel through 5 cm of compacted sand before release, *in situ* a large number of cells was transported into the upper slope of the ripples (Fig. 4) and then traveled on a short path through unconsolidated sediment towards the ripple crest where cells could again be released. The effect of this release became apparent after cell concentrations dropped in the water column resulting in the decline of concentrations in the sediment and visible organic particle stripes at the ripple crests. Concentrations of high

extracellular polymeric substances (EPS) in the sediment, or feeding benthos organisms, may enhance retention of organic particles in flushed permeable sands; however, these factors were apparently not effective at Hel during our study.

CONCLUSIONS

In the present study we have shown rapid temporal changes in algal abundance in permeable sublittoral sediment subjected to oscillating bottom flows. Under very calm conditions with only small waves and ensuing filtration rates of approximately 40 l m^2 d^{-1}, the sediments at the 3 stations would filter the entire overlying water column within 13, 25 and 38 d, respectively. *In situ* measurements in other sandy coastal sediments have shown that filtration can easily reach rates 10-fold as high, when the bottom currents are stronger due to higher waves or tidal currents (Reimers et al. 2004). This would reduce the time period for filtration of the entire overlying water column to a little more than 1 d at the shallowest station and about 4 d at the 1.5 m station. This underlines the potential importance of the shallow coastal sands for the removal of bloom organisms and coastal water quality.

However, sedimentary filtration effectively removes particles from the overlying water only if the sand can retain the organic particles carried into the bed. Filtered algae added only a relatively small amount to the sedimentary organic matter pool at our study site, probably primarily due to the short duration of the bloom in the bay and the flushing of trapped cells from the sediment as a consequence of relatively low retention efficiency. However, the *Peridinella catenata* cells represented highly degradable material that is delivered to the subsurface microbial community within hours of the arrival of the algal bloom. DOC generated during the sedimentary degradation of the algae was almost completely remineralized to DIC within the bed. Because the majority of the organic carbon in marine sediments is contained in refractory material and the organic grain coatings degraded at a very slow rate (Kristensen & Hansen 1995, Kristensen et al. 1995, Kristensen & Holmer 2001), a relatively small amount of labile organic matter delivered to the sediment, may still have a significant influence on the sedimentary microbial community.

Acknowledgements. We thank K. Skóra and the staff of the 'Hel Marine Station' for access to the station and their help in this project. S. Menger, M. Alisch, and A. Glud, are thanked for assistance in the field and the laboratory. GFDI at Florida State University in Tallahassee provided access to the flume facility, and we thank R. Kung, M. Higgs, and M. Laschet for their assistance with the flume work. Without the technical support of V. Meyer and G. Herz, this project would not have been possible. We thank B. B. Jørgensen and A. Boetius for supporting this study. This research was supported by the Max Planck Society, the European Commission (COSA project, EVK No. 3-CT-2002-00076), the Netherlands Institute of Ecology (PIONIER) and NSF grants 0424967 and 0536431. This is publication 3940 of the Netherlands Insitute of Ecology (NIOO-KNAW). Any opinions, findings, and conclusions or recommendations expressed in this material are those of the author(s) and do not necessarily reflect the views of the European Commission or the National Science Foundation.

LITERATURE CITED

Amos CL, Feeney T, Sutherland TF, Luternauer JL (1997) The stability of fine-grained sediments from the Fraser River delta. Estuar Coast Shelf Sci 45:507–524

Andersen FO (1996) Fate of organic carbon added as diatom cells to oxic and anoxic marine sediment microcosms. Mar Ecol Prog Ser 134:225–233

Andersen TK, Jensen MH, Sørensen J (1984) Diurnal variation of nitrogen cycling in coastal, marine sediments. I. Denitrification. Mar Biol 83:171–176

Burdige DJ, Zheng S (1998) The biogeochemical cycling of dissolved organic nitrogen in estuarine sediments. Limnol Oceanogr 43:1796–1813

Cook PLM, Wenzhöfer F, Glud RN, Huettel M (in press) Benthic solute exchange and carbon mineralization in two shallow subtidal sandy sediments: impact of advective porewater exchange. Limnol Oceanogr

Danovaro R, Armeni M, Dell'Anno A, Fabiano M, Manini E, Marrale D, Pusceddu A, Vanucci S (2001) Small-scale distribution of bacteria, enzymatic activities, and organic matter in coastal sediments. Microbial Ecology 42: 177–185

Dauwe B, Middelburg JJ, Herman PMJ (2001) Effect of oxygen on the degradability of organic matter in subtidal and intertidal sediments of the North Sea area. Mar Ecol Prog Ser 215:13–22

Ehrenhauss S, Huettel M (2004) Advective transport and decomposition of chain-forming planktonic diatoms in permeable sediments. J Sea Res 52:179–197

Ehrenhauss S, Witte U, Buhring SL, Huettel M (2004a) Effect of advective porewater transport on distribution and degradation of diatoms in permeable North Sea sediments. Mar Ecol Prog Ser 271:99–111

Ehrenhauss S, Witte U, Janssen F, Huettel M (2004b) Decomposition of diatoms and nutrient dynamics in permeable North Sea sediments. Cont Shelf Res 24:721–737

Falter JL, Sansone FJ (2000) Hydraulic control of porewater geochemistry within the oxic–suboxic zone of a permeable sediment. Limnol Oceanogr 45:550–557

Franke U, Polerecky L, Precht E, Huettel M (2006) Wave tank study of particulate organic matter degradation in permeable sediments. Limnol Oceanogr 51:1084–1096

Glibert PM, Harrison J, Heil C, Seitzinger S (2006) Escalating worldwide use of urea — a global change contributing to coastal eutrophication. Biogeochemistry 77:441–463

Harrison WD, Musgrave D, Reeburgh WS (1983) A wave-induced transport process in marine sediments. J Geophys Res 88:7617–7622

Haya K (1995) IOC-FAO intergovernmental panel on harmful algal blooms. UNESCO, Paris

Howarth RW, Sharpley A, Walker D (2002) Sources of nutrient pollution to coastal waters in the United States: implica-

tions for achieving coastal water quality goals. Estuaries 25:656–676

Hu CM, Muller-Karger FE, Taylor C, Carder KL, Kelble C, Johns E, Heil CA (2005) Red tide detection and tracing using MODIS fluorescence data: a regional example in SW Florida coastal waters. Remote Sens Environ 97: 311–321

Huettel M, Gust G (1992) Impact of bioroughness on interfacial solute exchange in permeable sediments. Mar Ecol Prog Ser 89:253–267

Huettel M, Rusch A (2000) Transport and degradation of phytoplankton in permeable sediment. Limnol Oceanogr 45:534–549

Huettel M, Webster IT (2000) Porewater flow in permeable sediment. In: Boudreau BP, Jørgensen BB (eds) The benthic boundary layer: transport processes and biogeochemistry. Oxford University Press, Oxford, p 144–179

Huettel M, Ziebis W, Forster S (1996) Flow-induced uptake of particulate matter in permeable sediments. Limnol Oceanogr 41:309–322

Huettel M, Ziebis W, Forster S, Luther GW (1998) Advective transport affecting metal and nutrient distributions and interfacial fluxes in permeable sediments. Geochim Cosmochim Acta 62:613–631

Huettel M, Roy H, Precht E, Ehrenhauss S (2003) Hydrodynamical impact on biogeochemical processes in aquatic sediments. Hydrobiologia 494:231–236

Jago CF, Jones SE (1998) Observation and modelling of the dynamics of benthic fluff resuspended from a sandy bed in the southern North Sea. Cont Shelf Res 18:1255–1282

Jahnke R, Rao A, Richards M, Jahnke D (2005) Unexpected denitrification in oxic shelf sands: a consequence of redox dynamics? Geochim Cosmochim Acta 69:A577–A577

Jones SE, Jago CF, Bale AJ, Chapman D, Howland RJM, Jackson J (1998) Aggregation and resuspension of suspended particulate matter at a seasonally stratified site in the southern North Sea: physical and biological controls. Cont Shelf Res 18:1283–1309

Klute A, Dirksen C (1986) Hydraulic conductivity and diffusivity: laboratory methods. In: Klute A (ed) Methods of soil analysis. Part 1. Physical and mineralogical methods. American Society of Agronomy, Madison, WI, p 687–734

Kranck K, Smith PC, Milligan TG (1996) Grain-size characteristics of fine-grained unflocculated sediments: 'multi-round' distributions. Sedimentology 43:597–606

Kristensen E, Hansen K (1995) Decay of plant detritus in organic-poor marine sediment — production-rates and stoichiometry of dissolved C-compound and N-compound. J Mar Res 53:675–702

Kristensen E, Holmer M (2001) Decomposition of plant materials in marine sediment exposed to different electron accepters (O^{-2}, NO_3^-, and SO_4^{2-}), with emphasis on substrate origin, degradation kinetics, and the role of bioturbation. Geochim Cosmochim Acta 65:419–433

Kristensen E, Ahmed SI, Devol AH (1995) Aerobic and anaerobic decomposition of organic matter in marine sediment: which is fastest? Limnol Oceanogr 40:1430–1437

Lohse L, Kloosterhuis HT, Vanraaphorst W, Helder W (1996) Denitrification rates as measured by the isotope pairing method and by the acetylene inhibition technique in continental shelf sediments of the North Sea. Mar Ecol Prog Ser 132:169–179

McCandliss RR, Jones SE, Hearn M, Latter R, Jago CF (2002) Dynamics of suspended particles in coastal waters (southern North Sea) during a spring bloom. J Sea Res 47: 285–302

Menden-Deuer S, Lessard EJ (2000) Carbon content and carbon:volume ratios of heterotrophic and autotrophic dinoflagellates. Limnol Oceanogr 45:569–579

Menzel DW, Vaccaro RF (1964) The measurement of dissolved organic and particulate carbon in seawater. Limnol Oceanogr 9:138–142

Middelburg JJ, Klaver G, Nieuwenhuize J, Vlug T (1995) Carbon and nitrogen cycling in intertidal sediments near Doel, Scheldt Estuary. Hydrobiologia 311:57–69

Moodley L, Middelburg JJ, Soetaert K, Boschker HTS, Herman PMJ, Heip CHR (2005) Similar rapid response to phytodetritus deposition in shallow and deep-sea sediments. J Mar Res 63:457–469

Niemi G, Wardrop D, Brooks R, Anderson S and 6 others (2004) Rationale for a new generation of indicators for coastal waters. Environ Health Perspect 112:979–986

Nixon SW (1995) Coastal marine eutrophication — a definition, social causes, and future concerns. Ophelia 41:199–219

Packman AI, Brooks NH (1995) Colloidal particle exchange between stream and stream bed in a laboratory flume. Mar Freshw Res 46:233–236

Packman AI, Brooks NH (2001) Hyporheic exchange of solutes and colloids with moving bed forms. Water Resour Res 37:2591–2605

Packman AI, Brooks NH, Morgan JJ (2000) Kaolinite exchange between a stream and streambed: laboratory experiments and validation of a colloid transport model. Water Resour Res 36:2363–2372

Paerl HW, Dennis RL, Whitall DR (2002) Atmospheric deposition of nitrogen: implications for nutrient over-enrichment of coastal waters. Estuaries 25:677–693

Pedersen AGU, Bernsten J, Lomstein BA (1999) The effect of eelgrass decomposition on sediment carbon and nitrogen cycling: a controlled laboratory experiment. Limnol Oceanogr 44:1978–1992

Pilditch CA, Emerson CW, Grant J (1998) Effect of scallop shells and sediment grain size on phytoplankton flux to the bed. Continental Self Research 17:1869–1885

Precht E, Huettel M (2003) Advective pore-water exchange driven by surface gravity waves and its ecological implications. Limnol Oceanogr 48:1674–1684

Precht E, Huettel M (2004) Rapid wave-driven advective porewater exchange in a permeable coastal sediment. J Sea Res 51:93–107

Reimers CE, Stecher HA, Taghon GL, Fuller CM, Huettel M, Rusch A, Ryckelynck N, Wild C (2004) In situ measurements of advective solute transport in permeable shelf sands. Cont Shelf Res 24:183–201

Riedl R, Huang N, Machan R (1972) The subtidal pump: a mechanism of intertidal water exchange by wave action. Mar Biol 13:210–221

Rusch A, Forster S, Huettel M (2001) Bacteria, diatoms and detritus in an intertidal sandflat subject to advective transport across the water–sediment interface. Biogeochemistry 55:1–27

Rusch A, Huettel M, Reimers CE, Taghon GL, Fuller CM (2003) Activity and distribution of bacterial populations in Middle Atlantic Bight shelf sands. FEMS Microbiol Ecol 44:89–100

Seitzinger SP, Kroeze C (1998) Global distribution of nitrous oxide production and N inputs in freshwater and coastal ecosystems. Global Biogeochem Cycles 12:93–113

Sims I (1993) Measuring the growth of phytoplankton: the relationship between total organic carbon with three commonly used parameters of algal growth. Arch Hydrobiol 128:459–466

Strickland JDH, Parsons TR (1972) A practical handbook of seawater analysis, 2nd edn. Bull Fish Res Board 167:1–310

Tomlinson MC, Stumpf RP, Ransibrahmanakul V, Truby EW, Kirkpatrick GJ, Pederson BA, Vargo GA, Heil CA (2004) Evaluation of the use of SeaWiFS imagery for detecting *Karenia brevis* harmful algal blooms in the eastern Gulf of Mexico. Remote Sens Environ 91:293–303

Verity PG, Stoecker DK, Sieracki ME, Burkill PH, Edwards ES, Tronzo CR (1993) Abundance, biomass and distribution of heterotrophic dinoflagellates during the North Atlantic spring bloom. Deep-Sea Res II 40:227–244

Webb JE, Theodor J (1968) Irrigation of submerged marine sands through wave action. Nature 220:682–685

Westrich JT, Berner RA (1984) The role of sedimentary organic matter in bacterial sulfate reduction: the G model tested. Limnol Oceanogr 29:236–249

Widdows J, Blauw A, Heip CHR, Herman PMJ and 6 others (2004) Role of physical and biological processes in sediment dynamics of a tidal flat in Westerschelde Estuary, SW Netherlands. Mar Ecol Prog Ser 274:41–56

Ziebis W, Forster S, Huettel M, Jorgensen BB (1996) Complex burrows of the mud shrimp *Callianassa truncata* and their geochemical impact in the sea bed. Nature 382: 619–622

Editorial responsibility: Otto Kinne (Editor-in-Chief), Oldendorf/Luhe, Germany

Submitted: July 25, 2006; Accepted: November 22, 2006
Proofs received from author(s): June 6, 2007